

## Effect of Elevated Temperatures on the Formability of AA2014 Thin-Walled Tube Ends

L. Venugopal, M. J. Davidson & N. Selvaraj

**To cite this article:** L. Venugopal, M. J. Davidson & N. Selvaraj (2013) Effect of Elevated Temperatures on the Formability of AA2014 Thin-Walled Tube Ends, Materials and Manufacturing Processes, 28:3, 319-323, DOI: [10.1080/10426914.2012.746785](https://doi.org/10.1080/10426914.2012.746785)

**To link to this article:** <https://doi.org/10.1080/10426914.2012.746785>



Published online: 07 Mar 2013.



Submit your article to this journal 



Article views: 157



View related articles 



Citing articles: 2 [View citing articles](#) 

## Effect of Elevated Temperatures on the Formability of AA2014 Thin-Walled Tube Ends

L. VENUGOPAL, M. J. DAVIDSON, AND N. SELVARAJ

*Department of Mechanical Engineering, National Institute of Technology, Warangal, India*

Thin-walled tubes are used in a number of industrial applications as interconnecting elements, in the pneumatic, hydraulic, and exhaust systems of machines, in the electrical and electronics industry, as connectors in medical devices etc. The end of the tubes should be formed into different shapes that will suit the need of the above mentioned applications. In most of the applications, the tube ends either will be expanded or converged. However, there is a limit to which these tubes are expanded or converged, which depends on the material property as well as the process used. In the present study, an effort has been made to expand tubes of AA2014 aluminum alloy, which is an aerospace alloy containing copper as one of its main constituent. Different heat treatment processes such as solutionizing, aging, and annealing have been done on the preform to enhance its formability. Due to the low ductility of AA2014 alloy, the tube has been expanded at elevated temperatures. Finite element analysis based simulation studies have been performed to minimize the number of experiments. The formability of the tube has been found to improve considerably at the elevated temperatures.

**Keywords** Aluminum; Compression; Deformation; Experimentation; Formability; Fracture; Model; Simulations.

### INTRODUCTION

End forming process is used to make complex shaped tube ends either by expanding or reducing the ends of the tubes. It finds application in the aerospace, automotive, construction, marine, medical, and military industries. The complex shapes in tube ends are achieved by pressing a dedicated die having the shape of the required profile either by a hydraulic or a mechanical press and the dedicated die will be retracted back after achieving the required shape. During the expansion process, the tube may fail prematurely before achieving its intended size and shape. The tube may either buckle or may tear on the tube edge.

Tube end forming process is governed by a number of process parameters, namely the punch/die cone angle, ratio between punch radius, and the initial reference radius, friction, punch speed, tube length, and tube thickness. To understand the process, only a small amount of literature pertaining to the process was studied. Alves et al. [1–2] investigated the expansion and reduction of thin-walled tubes using a die. The authors concluded that the process is only achievable with in a compact range of process parameters. Almeida et al. [3] performed theoretical and experimental investigations to understand the tube expansion and reduction processes. The authors analyzed the different modes of deformation and established formability principles. The authors performed tests on the naturally aged AA 6060 aluminum alloy to determine the formability

during tube expansion. They reported the critical plastic instability load and damage values for the occurrence of local buckling and ductile fracture, respectively. Schaeffer et al. [4] described in detail the various tube end forming processes such as expansion, reduction, internal inversion, and external inversion.

However, the information gained from the above references did not help much in the forming of AA2014 tubes and the response of the metal to cold forming was poor. A review on the literature revealed that no work has been reported on the tube expansion studies of AA2014 alloys. To analyze the influence of temperature on the formability of AA2014 tubes, the tube end forming of the alloy was performed at elevated temperatures. Several researches have used the elevated temperature route to achieve desired results. Brnic et al. [5] performed numerical analysis and creep studies to evaluate the performance of tool materials at elevated temperatures. De Flora et al. [6] performed hot wear and thermal fatigue resistance of 55NiCrMoV7 tool steel, which is used as a mandrel in ring rolling. The authors reported higher hardness of the steel at elevated temperatures. Mustafa et al. [7] used a drop-weight test rig to find the dynamic fracture strength and toughness of continuous alumina fiber-reinforced glass matrix composites at elevated temperatures. Sinclair et al. [8] analyzed the effect of preheating on the welding force reduction of friction stir-welded AA6061 alloys. The authors observed a 43% reduction in the axial force, when the work piece was preheated to 300°C. Bae et al. [9] analyzed the influence of temperature on the tribological behaviour of surface modified silicon carbide. Hole expansion ratio has been used to characterize the formability of hot-rolled high-strength steels [10]. The mechanical properties namely yield strength, ultimate

---

Received September 7, 2012; Accepted October 16, 2012

Address correspondence to L. Venugopal, Department of Mechanical Engineering, National Institute of Technology, Warangal, A.P., India-506004; E-mail: venugopal315@gmail.com

tensile strength, elongation, and carbon equivalent were correlated with the hole-expansion ratio of various grades of hot-rolled steel. The workability of AA7075 aluminum alloy reinforced with 15% of sic particles has been studies at elevated temperatures [11]. The processing map has been developed with the hot working process parameters namely, temperatures and strain rates. The crack forming conditions of two different duplex stainless steel with varying nitrogen contents of 0.22% and 0.18% were studied at elevated temperatures [12]. The alloy 0.22% nitrogen was found to crack in a temperature range of 1,050–1,100°C. Although several researchers have worked on the elevated temperature behavior of different alloys, no study has been reported on the tube end forming studies at elevated temperatures. In this article, the role of elevated temperatures on the tube end formability of AA2014 is discussed.

#### MATERIALS AND METHODS

The material used for the present investigation is AA2014 alloy. The experiments were performed on a hydraulic press of 50 ton capacity. The hydraulic press used in the present experiments is shown in Figs. 1a and b. The die was mounted on the ram. A constant ram speed of 0.5 mm/s was used. Before starting the test, the tube was adjusted in such a way that the axis of tube and punch were aligned. During the forming process, the load was increased by rotating the pressure valve manually. Punch displacements were measured using a LVDT. A PC-based data logging system was used to record and store the loads and displacements. The process was continued until the punch moved inside the tube fully or till the appearance of crack at the tube tip.

#### Experimental Work

The tube expansion study was performed both at cold and at elevated temperatures. For the cold forming

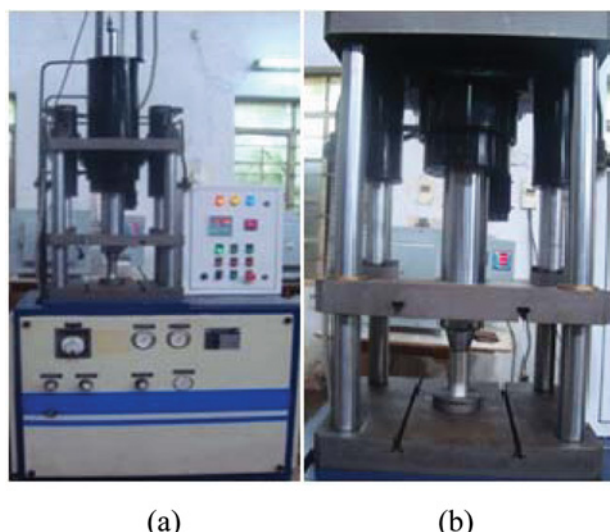


FIGURE 1.—(a) Hydraulic press; (b) test sample and die set (color figure available online).

TABLE 1.—Process parameters.

Heat treatment process	Temperature (°C)	Time (h)
Annealing	416	2
Solutionizing	502	2–6
Aging	160–180	2–48

experiments, a preform with 2 mm thickness and 90 mm length was expanded with a tool with  $r_p/r_o$  ratio of 1.57 and  $\alpha = 30^\circ$ , where  $r_p/r_o$  is the expansion ratio, in which “ $r_p$ ” is the punch radius at its top, “ $r_o$ ” is the punch radius at its bottom, and “ $\alpha$ ” is the forming angle or die cone angle. Dies of different expansion ratios namely 1.39, 1.53, and 1.67 and different cone angles like 15°, 30°, and 45° were made but the optimum of those was chosen for the present work. A linear expansion of 6 mm was obtained in the cold forming tests which is very low, due to the poor ductility of the alloy, at room temperature. Different heat treatments were tried on the tube preform to increase its formability. The tube was subjected to annealing, solutionizing, and aging treatments. Finite element analysis based simulations were performed to minimize the number of experiments. The process parameters that were utilized in the experiments are given in Table 1.

#### FEA Simulations

DEFORM 2D software was used to perform the simulation study. The material property data related to AA2014 at various heat treated state was found out by performing disc compression tests at the annealed state, solutionized state, and the aged state (done at different aging times). The strain hardening index, “ $n$ ,” and strength coefficient, “ $k$ ,” were found from the above tests and these values were used in the flow curve of DEFORM 2D package. Tube expansion simulations were then performed on the alloy with their respective “ $n$ ” and “ $k$ ” values and the linear and radial expansion were measured. The “ $n$ ” and “ $k$ ” values for different heat treated states are given in Table 2.

#### Ring Compression Test

The forming load can be successfully reduced by employing lubricants in the tool work piece interface. For the present case, the friction condition at the tube-die interface was estimated by performing ring compression tests. The test samples were taken in the ratio of 6:3:2, i.e., OD = 18 mm, ID = 9 mm, and Height = 6 mm. The ring samples were compressed to various height reductions in a 50 ton hydraulic press. The inside and outside diameter and height of the ring specimen before and after deformation were measured. A graph was drawn between the percentage reduction in height and the percentage reduction in diameter for each of the samples with different lubricants.

The mean value of the change in the hole diameter to the height reduction of all the specimens gives the value of the friction coefficient “ $m$ .” For the condition of no

TABLE 2.—The measured “n” and “K” values for different heat treatment processes from disc compression tests.

Heat treatment	n	K	Linear displacement (mm)	Radial expansion (mm)	Load (KN)
Base material	0.12	699	6	42.18	24
Air cooling	0.23	528	7	43.48	17.5
Furnace cooling	0.26	424	7	43.46	13.2
2 h ST	0.13	714	6	42.22	24.3
2 h ST, 2 h AT	0.11	828	6	42.18	28.6
2 h ST, 24 h AT	0.10	714	6	42.16	25.7
2 h ST, 48 h AT	0.11	712	6	42.22	24.5
6 h ST	0.17	843	7	43.34	35.3
6 h ST, 6 h AT	0.12	854	6	42.12	28.8
6 h ST, 24 h AT	0.11	749	6	42.16	26.7
6 h ST, 48 h AT	0.10	705	6	42.12	28.4
5 h ST, 7 h AT	0.16	1396	6	42.12	40.8

ST: Solution Time; AT: Aging Time.

friction between the tube-work piece interface, the friction coefficient is taken as  $m=0$  and for sticking condition the “m” value is taken as 1. Low friction causes the ring hole to expand whereas high friction causes the hole to bulge. The “m” value for grease, molybdenum disulphide, white grease, palm oil, and dry lubrication is found to be 0.2, 0.3, 0.4, 0.5, and 0.55, respectively, as illustrated in Fig. 2a. Figures 2b and c shows the compressed ring samples and the sample dimension. MoS<sub>2</sub> was found to be effective in reducing the load compared to other lubricants.

## RESULTS AND DISCUSSION

### Critical Damage

DEFORM 2D uses Cockcroft & Latham algorithm to predict failure. The failure stress is given by damage factor. The damage factor increases as a material is deformed. Fracture occurs when the damage factor reaches its critical value. The critical value of the damage factor is determined through experiments. Damage factor,  $D_f$ , of Cockcroft & Latham algorithm is defined

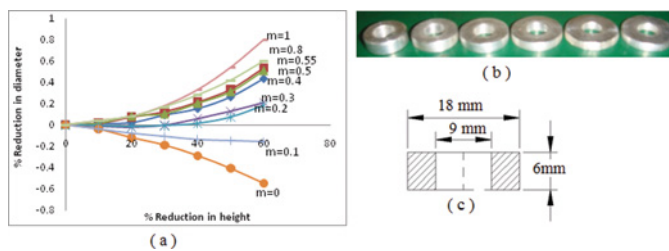


FIGURE 2.—Determination of friction value from ring compression tests. (a) Calibration curves; (b) ring compressed samples at different height reductions; (c) dimensions of ring specimen (color figure available online).

by Eq. (1):

$$D_f = \int \frac{\sigma^*}{\sigma} d\epsilon, \quad (1)$$

where  $\sigma^*$  is the maximum tensile principal stress,  $\sigma$  is the effective stress and  $d\epsilon$  is the effective strain increment. The tube was expanded until its failure in the hydraulic press and the same was redone on the simulation package, DEFORM 2D, and the run was stopped at the strain level corresponding to the experimental strain value at which the tube failed. The damage factor corresponding to this strain value has been taken as the critical damage factor and it was found to be 0.112.

### Effect of Heat Treatment

Extensive simulation studies were performed on DEFORM 2D with the simulated alloy having material property evaluated from different disc compression tests at several heat treatment states such as annealing, solution treatment and aging. The linear displacement and radial expansion of the expanded tubes were measured. The linear displacement is the distance by which the tube has been expanded by the die from the tip of the tube to the point where the die expands along the die cone angle, measured along the length of the axis of the tube. Radial expansion is the increase in diameter of the tube by the die measured on the top most portion of the tube across its circumference. It was found that there was only marginal increase in the expansion due to heat treatment. Even though the solutionizing treatment made the material soft, it resulted in buckling of the tube. Even though the artificial aging treatment improved the strength of the material, and the load bearing capacity of the preform improved, it did not result in the improvement of the radial expansion.

### Hot Forming

As AA 2014 alloy has exhibited poor formability at room temperature, the elevated temperature forming route has tried to improve its formability. In hot forming process, the metal gets softened and the formability is improved. A heating chamber was made and was kept on the table of the hydraulic press. Enough space was provided on the furnace to hold the bottom die and the work piece. An opening was provided on the top of the furnace to enable the movement of the ram with the top die to enter inside and to expand the tube. The top of the furnace was closed with glass wool and the tube samples were heated to different temperatures namely 100, 150, 200, 250, 300, 350, 400, 450, and 500°C. The tubes were expanded with a die of  $r_p/r_o$  ratio of 1.57 and  $\alpha = 30^\circ$ . The same process parameters were employed for all the elevated temperature tests shown in Fig. 3. During the tests, the temperature of specimen was kept at constant until the tube was stretched to failure. The load and displacement values obtained at different temperatures are given in Table 3. The simulations performed at different temperatures are shown in

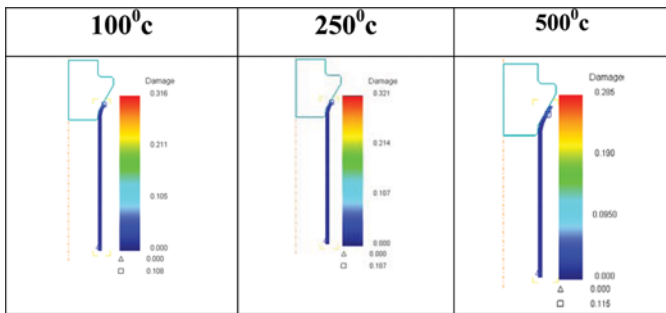


FIGURE 3.—Tube end forming simulations at different temperatures (color figure available online).

Fig.3. With increase in temperature, the tube was found to expand more and the forming load decreased. No visible improvement was seen up to a temperature of 250°C. The formability increased to a maximum at a forming temperature of 500°C.

To further improve the formability, the tube was subjected to different cycles of annealing treatment. A linear displacement of 6.1 mm was obtained in the cold condition and it improved to 9.9 mm when formed at a temperature of 450°C. Before the onset of failure, the tube was removed from the experimental set up and was annealed at a temperature of 416°C. The tube was expanded again with the die. A further linear displacement of 9.5 mm was achieved and the tube was subjected to another cycle of an annealing treatment which improved the linear displacement by another 4.6 mm before failure. Thus, a total displacement of 24 mm was achieved at the end of the second annealing cycle. In all the above cases, the tube was expanded at 450°C after annealing treatment. Table 4 gives the

TABLE 3.—The load-displacement values obtained at different temperatures.

Temperature (°C)	Displacement (mm)	Load (KN)
100	6.00	13.7
150	6.00	11.8
200	6.00	10.0
250	6.00	6.20
300	6.50	9.50
350	8.00	5.80
400	8.00	4.10
450	9.50	4.30
500	13.0	6.40

TABLE 4.—Displacement values for the tube end processed tubes for various process conditions.

Process condition	Linear displacement (mm)
Cold forming (A)	06.1
Hot forming without cracking (C)	09.9
Hot forming with crack (B)	11.0
Hot forming with 1st stage annealing (D)	19.4
Hot forming with 2nd stage annealing (E)	24.0



FIGURE 4.—Samples of AA2014 alloy tubes at different heat treatment and forming stages ( $r_p/r_o$  ratio = 1.57 and  $\alpha = 30^\circ$ ) (color figure available online).

displacement values of the tube for the various heat-treated conditions. The tubes were expanded with a die with  $r_p/r_o$  ratio of 1.57 and  $\alpha = 30^\circ$ . Figure 4 shows the tube samples of AA2014 alloy expanded by the conical punch in the cold forming process, hot forming process with crack, hot forming process without crack, hot forming after first stage of annealing, and hot forming process after second stage of annealing, respectively. The cold formed tube is given for comparison. In all the cases shown above, a die with  $r_p/r_o$  ratio of 1.57 and  $\alpha = 30^\circ$  was used. The hot forming test performed up to the onset of crack was done at a temperature of 450°C to arrive at its limiting strain. Figure 4a shows the tube that was expanded at room temperature and Fig.4b shows the tube that was expanded till it cracked. Figure 4c shows the tube, the forming of which was stopped just before the onset of failure. This was done to use the tube for subsequent annealing treatment. Figures 4d and e show the tubes expanded after annealing treatment. The annealing was done at a temperature of 416°C and the subsequent forming was done at a temperature of 450°C. Figure 4d shows the tube expanded after a single annealing stage and Fig. 4e shows the tube expanded after two stages of annealing. The second annealing was done after the tube was expanded up to 19.4 mm.

## CONCLUSIONS

Experimental and simulation studies on AA2014 tubes were performed by expanding the tubes to different temperatures. The main conclusions from this study are listed below.

1. The experiments revealed that the tube failed after reaching a radial expansion of 6.1 mm in the cold condition.
2. To improve the formability an attempt was made to change the material property by subjecting the material to heat treatment. Only minor change in the expansion could be achieved by the heat treatment.
3. No visible improvement in formability was seen up to a temperature of 250°C while the formability increased to a maximum at a temperature of 500°C.
4. To further improve the formability, the tube was subjected to different cycles of annealing treatment.

The tube failed after reaching a radial expansion of 6.1 mm in the cold condition. It improved to 9.9 mm when formed at a temperature of 450°C. Different cycles of annealing were performed on the tubes and the tubes expanded to 24 mm at the end of the second stage of annealing treatment.

5. The finite element results obtained from the simulations predicted the expansion values accurately and it can be used for further studies.

#### ACKNOWLEDGMENTS

The authors would like to thank the Department of Science and Technology, Govt. of India, for the financial support under the Young Scientist Scheme (SR/FT/Et-071/2008 dated May 21, 2009) to Dr. M. J. Davidson.

#### REFERENCES

1. Alves, M.L.; Almeida, B.P.P.; Rosa, P.A.R.; Martins, P.A.F. End forming of thin-walled tubes. *Journal of Material Processing Technology* **2006**, *177*, 183–187.
2. Alves, L.M.; Martins, P.A.F. Cold expansion and reduction of thin-walled PVC tubes using a die. *Journal of Material Processing Technology* **2009**, *209*, 4229–4236.
3. Almeida, B.P.P.; Alves, M.L.; Rosa, P.A.R.; Brito, A.G.; Martins, P.A.F. Expansion and reduction of thin-walled tubes using a die: Experimental and theoretical investigation. *International Journal of Machine Tools and Manufacture* **2006**, *46*, 1643–1652.
4. Schaeffer, L.; Brito, A.M.G. FEM Numerical simulation and experimental investigation on end forming of thin-walled tubes using a die. *Steel Research International* **2007**, *78*, 10–11.
5. Brnic, J.; Canadija, M.; Turkalj, G.; Lanc, D.; Pepelnjak, T.; Barisic, B.; Vukelic, G.; Brcic, M. Tool material behavior at elevated temperatures. *Materials and Manufacturing Processes* **2009**, *24* (7–9), 758–762.
6. De Flora, M.G.; Pellizzari, M. Behavior at elevated temperature of 55nicrmov7 tool steel. *Materials and Manufacturing Processes* **2009**, *24* (7–8), 791–795.
7. Mustafa, R.J.; Al-Hamdan, A.A.; Nimir, Y.L. Dynamic fracture strength and toughness of continuous alumina fiber-reinforced glass matrix composites at elevated temperature. *Materials and Manufacturing Processes* **2011**, *26*, 579–585.
8. Sinclair, P.C.; Longhurst, W.R.; Cox, C.D.; Lammlein, D.H.; Strauss, A.M.; Cook, G.E. Heated friction stir welding: an experimental and theoretical investigation into how preheating influences process forces. *Materials and Manufacturing Processes* **2010**, *25*, 1283–1291.
9. Bae, H-T.; Choi, H-J.; Jeong, J-H.; Lim, D-S. The effect of reaction temperature on the tribological behavior of the surface modified silicon carbide by the carbide derived carbon process. *Materials and Manufacturing Processes* **2010**, *25* (5), 345–349.
10. De, S.K.; Deva, A.; Mukhopadhyay, S.; Jha, B.K. Assessment of formability of hot rolled steel through determination of hole-expansion ratio. *Materials and Manufacturing Process* **2011**, *26* (1), 37–42.
11. Rajamuthamilselvan, M.; Ramanathan, S. Hot-working behavior of 7075 Al/15% SiC<sub>p</sub> composites. *Materials and Manufacturing Process* **2012**, *27* (3), 260–266.
12. Manikanda Subramanian, K.; Chandramohan, P. Crack formation during hot rolling of nitrogen alloyed duplex stainless steel. *Materials and Manufacturing Process* **2012**, *27* (9), 996–1000.